Structure and Stability of [VO2]+ in Aqueous Solution: A Car−Parrinello and Static Ab Initio Study. (lien)

ARTICLE *in* INORGANIC CHEMISTRY · JULY 2007

Impact Factor: 4.76 · DOI: 10.1021/ic0614519 · Source: PubMed

7 AUTHORS, INCLUDING:

Aymeric Sadoc
University of Nantes
16 PUBLICATIONS **192** CITATIONS
SEE PROFILE

Eric Furet
Ecole Nationale Supérieure de Chimie de Re…
52 PUBLICATIONS **495** CITATIONS
SEE PROFILE

Régis Gautier
Ecole Nationale Supérieure de Chimie de Re…
127 PUBLICATIONS **738** CITATIONS
SEE PROFILE

Eric Le Fur
Ecole Nationale Supérieure de Chimie de Re…
71 PUBLICATIONS **371** CITATIONS
SEE PROFILE

Inorg. Chem. **2007**, *46*, 4835–4843

Structure and Stability of VO_2^+ in Aqueous Solution: A Car–Parrinello and Static ab Initio Study

Aymeric Sadoc, Sabri Messaoudi, Eric Furet,* Régis Gautier, Eric Le Fur, Laurent le Pollès, and Jean-Yves Pivan

UMR CNRS 6226-Sciences Chimiques de Rennes, Ecole Nationale Supérieure de Chimie de Rennes, Campus de Beaulieu, Avenue du Général Leclerc, 35700 Rennes, France

Received August 2, 2006

Quantum chemical calculations have been carried out to get some insight concerning the effects of temperature and solvent acidity on the structure and stability of solvated VO_2^+ as the elementary chemical unit involved in the nucleation of vanadophosphates. First, because some recent theoretical studies have suggested a tendency of density functional theory (DFT) to favor lower coordination numbers for such systems, static calculations have been performed on $[VO_2(H_2O)_{(4-n)}]^+ \cdot nH_2O$ ($n = 0$–2) conformers at the MP2 and DFT level of theory, using two different combinations of basis sets. The results of two pure-GGA (BP86 and PBEPBE), two hybrid-GGA (PBE1PBE and mPWPW91), and two hybrid-meta-GGA (mPW1B95 and B1B95) functionals were analyzed on these systems. The comparison of the results indicates that the stability differences between the two methodologies are resolved when hydration energy is taken into account, provided that some amount of HF exchange is introduced in the DFT calculations. In a second step, Car–Parrinello simulations have been carried out starting from $VO_2(H_2O)_4^+$ surrounded by water molecules. The calculations at 300 K show the natural tendency of $VO_2(H_2O)_4^+$ to decompose to $VO_2(OH)_2^-$ and the requirements to work with an already acidified medium to be able to investigate the coordination sphere of VO_2^+ for an extended period of time. Under such conditions, we have obtained a clear preference for a five-coordinated vanadium. The molecular dynamics simulations performed at 500 K starting from hydrated VO_2^+ in a protonated medium found $VO(OH)_3$ to be the most stable structure, whereas this ideal candidate for oxolation reactions is expected to be a very minor species at room temperature.

Introduction

Vanadium in its V+ oxidation state exhibits a rich aqueous chemistry for which, as shown in Figure 1, the detected species are strongly dependent upon the pH and vanadium concentration. Indeed, this system is characterized by numerous equilibria associated with hydrolysis and polymerization reactions where various mono- and polynuclear entities are involved.[1] The aqueous chemistry of V(V+) can be related to those of W and Mo d^0 for which several isopolymetalates have also been identified.[2] Analogies with phosphate have also been reported both from the structural point of view

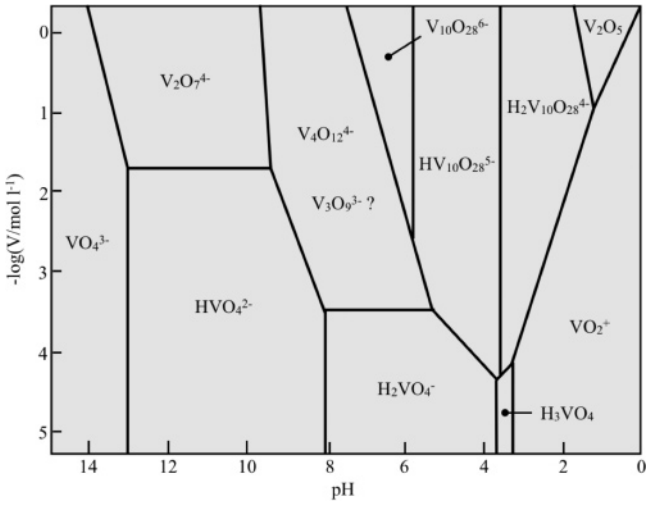

Figure 1. Stability domains of various vanadates and polyvanadates as a function of the pH and vanadium concentration.

* To whom correspondence should be addressed. E-mail: eric.furet@ensc-rennes.fr.

(1) Greenwood, N. N.; Earnshaw, A. Vanadium, Niobium and Tantalum. *Chemistry of the Elements*; Butterworth Heinemann: Oxford, U.K., 1998.

(2) Richens, D. T. *The Chemistry of Aqua Ions: Synthesis, Structure, and Reactivity: A Tour through the Periodic Table of the Elements*; Wiley: Chichester, U.K., 1997.

10.1021/ic0614519 CCC: $37.00
Published on Web 05/11/2007

(oligomers formation) and concerning electronic properties (pKa values of phosphate and vanadate systems). They were notably used to explain the biological effects of aqueous solutions containing vanadate mixtures.[3]

At both sides of the pH scale (Figure 1), the monomeric units VO_2^+ and VO_4^{3-} are predominant. For sufficiently high vanadium concentrations, solutions of those species may both lead by acidification or alkalinization, respectively, to the decavanadate $[V_{10}O_{28}]^{6-}$, which corresponds to a remarkable process. VO_2^+ and VO_4^{3-} and the protonation equilibria that connect them for concentrations lower than 2×10^{-5} M have been the subject of several experimental studies leading sometimes to different conclusions.[4−13] Harnung et al.[14] suggested an increase of the coordination number from 4 to 5 during the protonation step of HVO_4^{2-}, because of similarities in the spectra (^{51}V NMR and UV−visible) of binuclear complexes of V(V+) and $H_2VO_4^-$. In a later study, Cruywagen et al.[15] concluded from thermodynamic data that the expansion of the coordination sphere from 4 to 6 ligands occurs when the cation is formed and the formula $VO_2(H_2O)_4^+$ was suggested. The comparison of their results with those previously obtained on MoO_4^{2-} was used to support their conclusions, because a similar mechanism was previously established in the protonation step of $MoO_3(OH)^-$. Moreover, the data collected on the successive protonation equilibria of VO_4^{3-} lead them to cast some doubt on the existence of $VO(OH)_3$ to obtain satisfactory results for the calculation of the reaction constants. A similar conclusion was formulated by Pettersson et al.[9] as well as Larson[16] in earlier experimental studies.

From the point of view of one of our current projects devoted to rationalizing the condensation of vanadium ions in hydrothermal conditions, this last species is, however, the ideal candidate. Indeed, $VO(OH)_3$ possesses the maximum number of hydroxyl ligands with respect to the other mononuclear V(V+) species. Therefore, it is possible to suggest a theoretical mechanism for the formation of a prototypical compound such as $VOPO_4 \cdot 2H_2O$, because three V−O−P bridges can be readily formed through oxolation reactions.

To our knowledge, only one computational study, carried out by Bühl and Parrinello, has been devoted to some dynamical aspects of the aqueous chemistry of this family of mononuclear vanadates.[17] They investigated the influence of solvent effects on the ^{51}V chemical shifts in $VO_2(OH)_2^-$, VO_2^+, and $VO(O_2)(H_2O)^-$. As noted by the authors, simulations up to 2.5 ps, carried out at 300 K using Troullier−Martins pseudopotentials, were sufficient to compute dynamically averaged $\delta(^{51}V)$ values. For VO_2^+ specifically, the calculations using the BLYP functional allowed them to suggest a coordination number close to 5 and 5.5 in solution and in vacuo, respectively.

The primary aim of the present study is to carry out an investigation on the structure and stability of VO_2^+ focusing on the influence of factors such as the temperature or the acidity of the medium to gain insight into the behavior of solvated V(V) in conditions that mimic those found during the hydrothermal synthesis of vanadophosphates. Because some recent theoretical studies[18,19] have suggested that density functional theory (DFT) calculations would tend to overstabilize lower coordination numbers, we will describe, as a preliminary step, static DFT and MP2 calculations to analyze the influence of the computational method on the relative stability of various hydrated VO_2^+ conformers.

Computational Details

Static calculations were performed with the *Gaussian03*, revision B.04, package[20] to optimize geometries without constraints and compute frequencies. Six different combinations of exchange and correlation functionals were employed, corresponding to various levels of approximation along the DFT "Jacob's ladder", namely, BP86[21] and PBEPBE[22] for the pure functionals, PBE1PBE[23] and mPW1PW91[24] for the hybrid ones, and finally mPW1B95[25] and B1B95[26] as members of the hybrid-meta-GGA functionals family. Two combinations of basis sets have been employed. In the combination denoted ***A***, we used the 6-311+G(d) basis set[27,28] on vanadium and 6-31+G(d)[28,29] on oxygen and hydrogen. In the ***B***

(3) Crans, D. C.; Smee, J. J.; Gaidamauskas, E.; Yang, L. *Chem. Rev.* **2004**, *104*, 849.
(4) Cruywagen, J. J.; Heyns, J. B. B.; Westra, A. N. *Inorg. Chem.* **1996**, *35*, 1556.
(5) Cruywagen, J. J.; Heyns, J. B. B. *Polyhedron* **1991**, *10*, 249.
(6) Dyrssen, D.; Sekine, T. *J. Inorg. Nucl. Chem.* **1964**, *26*, 981.
(7) Rieger, P. H. *Aust. J. Chem.* **1973**, *26*, 1173.
(8) Heath, E.; Howarth, O. W. *J. Chem. Soc., Dalton Trans.* **1981**, 1105.
(9) Pettersson, L.; Hedman, B.; Nenner, A.-M.; Andersson, I. *Acta Chem. Scand.* **1985**, *39*, 499.
(10) Pettersson, L.; Andersson, I.; Hedman, B. *Chem. Scr.* **1985**, *25*, 309.
(11) Ivakin, A. A.; Kurbatova, L. D.; Kruchinina, M. V.; Medvedeva, N. I. *Russ. J. Inorg. Chem. (Engl. Transl.)* **1986**, *31*, 219.
(12) Cruywagen, J. J.; Heyns, J. B. B.; Visagie, J. L. *Polyhedron* **1989**, *8*, 1800.
(13) Elvingson, K.; Fritzsche, M.; Rehder, D.; Pettersson, L. *Acta Chem. Scand.* **1994**, *48*, 878.
(14) Harnung, S. E.; Larsen, E.; Pederson, E. J. *Acta Chem. Scand.* **1993**, *47*, 674.
(15) Cruywagen, J. J.; Heyns, J. B. B.; Westra, A. N. *Inorg. Chem.* **1996**, *35*, 1556.
(16) Larson, J. W. *J. Chem. Eng. Data* **1995**, *40*, 1276.
(17) Bühl, M.; Parrinello, M. *Chem.−Eur. J.* **2001**, *7*, 4487.
(18) Diaz, N.; Suarez, D.; Merz, K. M. *Chem. Phys. Lett.* **2000**, *326*, 288.
(19) Rotzinger, F. P. *Chem. Rev.* **2005**, *105*, 2003.
(20) Frisch, M. J.; Trucks, G. W.; Schlegel, H. B.; Scuseria, G. E.; Robb, M. A.; Cheeseman, J. R.; Montgomery, J. A., Jr.; Vreven, T.; Kudin, K. N.; Burant, J. C.; Millam, J. M.; Iyengar, S. S.; Tomasi, J.; Barone, V.; Mennucci, B.; Cossi, M.; Scalmani, G.; Rega, N.; Petersson, G. A.; Nakatsuji, H.; Hada, M.; Ehara, M.; Toyota, K.; Fukuda, R.; Hasegawa, J.; Ishida, M.; Nakajima, T.; Honda, Y.; Kitao, O.; Nakai, H.; Klene, M.; Li, X.; Knox, J. E.; Hratchian, H. P.; Cross, J. B.; Bakken, V.; Adamo, C.; Jaramillo, J.; Gomperts, R.; Stratmann, R. E.; Yazyev, O.; Austin, A. J.; Cammi, R.; Pomelli, C.; Ochterski, J. W.; Ayala, P. Y.; Morokuma, K.; Voth, G. A.; Salvador, P.; Dannenberg, J. J.; Zakrzewski, V. G.; Dapprich, S.; Daniels, A. D.; Strain, M. C.; Farkas, O.; Malick, D. K.; Rabuck, A. D.; Raghavachari, K.; Foresman, J. B.; Ortiz, J. V.; Cui, Q.; Baboul, A. G.; Clifford, S.; Cioslowski, J.; Stefanov, B. B.; Liu, G.; Liashenko, A.; Piskorz, P.; Komaromi, I.; Martin, R. L.; Fox, D. J.; Keith, T.; Al-Laham, M. A.; Peng, C. Y.; Nanayakkara, A.; Challacombe, M.; Gill, P. M. W.; Johnson, B.; Chen, W.; Wong, M. W.; Gonzalez, C.; Pople, J. A. *Gaussian03*, revision B.04; Gaussian, Inc.: Wallingford, CT, 2004.
(21) (a) Becke, A. D. *Phys. Rev. A.: At., Mol., Opt. Phys.* **1988**, *38*, 3098. (b) Perdew, J. P. *Phys. Rev. B: Condens. Matter* **1986**, *33*, 8822.
(22) (a) Perdew, J. P.; Burke, K.; Ernzerhof, M. *Phys. Rev. Lett.* **1996**, *77*, 3865. (b) Perdew, J. P.; Burke, K.; Ernzerhof, M. *Phys. Rev. Lett.* **1997**, *78*, 1396.
(23) (a) Enzerhof, M.; Scuseria, G. E. *J. Chem. Phys.* **1999**, *110*, 5029. (b) Adamo, C.; Cossi, M.; Barone, V. J. *Mol. Struct. (THEOCHEM)* **1999**, *493*, 145.
(24) Adamo, C.; Barone, V. *J. Chem. Phys.* **1998**, *108*, 664.
(25) Zhao, Y.; Truhlar, D. G. *J. Phys. Chem. A* **2004**, *108*, 6908.
(26) Becke, A. D. *J. Chem. Phys.* **1996**, *104*, 1040.

basis-sets combination, we employed the TZVPP[30] basis set on vanadium and aug-cc-pVDZ[31] on oxygen and hydrogen. The effect of hydration was taken into account through the polarizable continuum model (CPCM)[32] as implemented in *Gaussian03*, and the calculations have been performed on the gas-phase geometries.

All of the Car−Parrinello molecular dynamics[33] simulations were performed using the *CPMD-3.9.2* program,[34] the Perdew−Becke−Ernzerhof[22] functional, an expansion of the plane-wave basis sets up to a kinetic energy cutoff of 30 Ry, and Vanderbilt ultrasoft pseudopotentials[35] generated with the USPP-7.3.4 program. For the vanadium pseudopotential only, we made use of a small core including the 1s, 2s, and 2p states. This pseudopotential was generated with V(0) as the all-electron reference state, incorporates a nonlinear core correction, and makes use of two s, two p, and two d nonlocal projectors. Results with the pseudopotentials employed are given in the Supporting Information. A periodic cubic box with 9.8692 Å side length was employed. The integration step was chosen to be equal to 0.121 fs (5 au), and hydrogen was replaced by deuterium to allow for such a time step. The fictitious electronic mass was selected to be equal to 600 au.

Results and Discussion

During our gas-phase dynamic test simulations using ultrasoft pseudopotentials starting from $VO_2(H_2O)_4^+$ (**H**), we obtained, as previously noted by Bühl and Parrinello,[17] a rapid evolution toward a pentacoordinated structure where one of the two most labile water molecules located trans to the oxo is decoordinated from the vanadium. This structure will be denoted here as $\mathbf{P_T}$ because the leaving ligand is bonded in a terminal fashion to one of the axial water molecules. Additionally, an alternative minor five-coordinated structure ($\mathbf{P_P}$), with the activated ligand bridging two water molecules, has also been optimized. Finally, a tetrahedral system (**T**) was computed because several significant lengthenings of $V-H_2O$ have been noted in $[VO_2(H_2O)_3]^+\cdot H_2O$. Table 1 summarizes the relative energies with respect to the hexacoordinated species computed in the gas phase using the ***A*** basis-sets combination (Computational Details section). It is immediately seen that the results of the two methods are completely different concerning the relative stabilities of the different conformers. Indeed, at the PBEPBE/***A*** level of theory, the energy ordering is $\mathbf{P_P} < \mathbf{T} \approx \mathbf{P_T} < \mathbf{H}$, with a difference $\mathbf{P_P} - \mathbf{H}$ of approximately 3.2 kcal/mol. However, the MP2 calculations conclude to a hexacoordinated preferred structure and a gap between the two extremes of more than 11 kcal/mol.

Table 1. Relative Energies (ΔE), Enthalpies ($\Delta H°$), and Free Energies ($\Delta G°$) Computed at the PBEPBE/***A*** and MP2/***A*** Levels of Theory for $[VO_2(H_2O)_{(4-n)}]^+\cdot nH_2O$ ($n = 0-2$)[a]

	H	$\mathbf{P_P}$	$\mathbf{P_T}$	T
PBEPBE				
ΔE	0.00	−3.18	−2.05	−2.23
$\Delta H°$	0.00	−3.14	−2.76	−3.86
$\Delta G°$	0.00	−2.67	−2.63	−5.67
MP2				
ΔE	0.00	1.41	5.73	11.09
$\Delta H°$	0.00	0.84	5.01	9.65
$\Delta G°$	0.00	−0.13	2.45	4.38

[a] Values are given in kcal/mol.

Table 2. Relative Energies (ΔE), Enthalpies ($\Delta H°$) and Free Energies ($\Delta G°$) Computed at the PBEPBE/***B*** and MP2/***B*** Levels of Theory for $[VO_2(H_2O)_{(4-n)}]^+\cdot nH_2O$ ($n = 0-2$)[a]

	H	$\mathbf{P_P}$	$\mathbf{P_T}$	T
PBEPBE				
ΔE	0.00	−3.83	−3.36	−5.18
$\Delta H°$	0.00	−3.82	−4.10	−6.75
$\Delta G°$	0.00	−2.99	−3.71	−8.24
MP2				
ΔE	0.00	0.20	3.10	8.40
$\Delta H°$	0.00	−0.38	3.22	6.84
$\Delta G°$	0.00	−0.83	1.51	2.57

[a] Values are given in kcal/mol.

Taking into account the zero-point, thermal, and entropic energy corrections induces with respect to **H** a stabilization that increases upon lowering of the coordination number for both kinds of calculations. The only exception is the $\mathbf{P_P}$ structure using DFT. This phenomenon leads to a noticeable preference for tetrahedral arrangement with the PBEPBE functional, an equivalent stability of **H** and $\mathbf{P_P}$ at the MP2 level, and a strong decrease of more than 6.5 kcal/mol for the energy difference $\mathbf{H} - \mathbf{T}$ in that case (Table 1). Therefore, it seems that a lower coordination number is preferred by DFT calculations, as suggested by Diaz et al.[18] in their theoretical investigation of Zn_2^+ solvation using both B3LYP and MP2. They also showed that their results were sensitive to computational parameters such as the basis-set quality. Therefore, we have reoptimized our geometries using the TZVPP basis set on vanadium and aug-cc-pVDZ otherwise, here noted as ***B***. Table 2 gathers the relative energies computed for the corresponding study. From the total energy point of view, the MP2 stability ordering appears to be unaffected, with, however, a difference $\mathbf{H} - \mathbf{P_P}$ that can now be considered as insignificant. Concerning the PBEPBE calculations, we obtain the sequence $\mathbf{T} < \mathbf{P_P} \approx \mathbf{P_T} < \mathbf{H}$. The previously noted differential stabilizations due to the correcting terms induce perturbations nearly equivalent to those reported with the ***A*** basis-sets combination. Therefore, we obtain the $\mathbf{P_P} < \mathbf{H} < \mathbf{P_T} < \mathbf{T}$ and $\mathbf{T} < \mathbf{P_T} < \mathbf{P_P} < \mathbf{H}$ orderings at the MP2 and DFT levels of theory, respectively, a reduction of the energy gap between the extremes with the perturbational method and a significant increase in the case of the PBEPBE functional with respect to the previous results. In the gas phase, we therefore have a preference for completely different structures depending on the theoretical model used, none of them corresponding to the hexacoordinated geometry suggested experimentally. The

(27) (a) Wachters, A. J. H. *J. Chem. Phys.* **1970**, *52*, 1033−1036. (b) Hay, P. J. *J. Chem. Phys.* **1977**, *66*, 4377−4384.
(28) Clark, T.; Chandrasekhar, J.; Spitznagel, G. W.; Schleyer, P. v. R. *J. Comput. Chem.* **1983**, *4*, 294−301.
(29) (a) Hehre, W. J.; Ditchfield, R.; Pople, J. A. *J. Chem. Phys.* **1972**, *56*, 2257−2261. (b) Hariharan, P. C.; Pople, J. A. *Theor. Chim. Acta* **1973**, *28*, 213−222.
(30) Schaefer, A.; Huber, C.; Ahlrichs, R. *J. Chem. Phys.* **1994**, *100*, 5829.
(31) (a) Dunning, T. H., Jr. *J. Chem. Phys.* **1989**, *90*, 1007. (b) Kendall, R. A.; Dunning, T. H., Jr.; Harrison, R. J. *J. Chem. Phys.* **1992**, *96*, 6769.
(32) Barone, V.; Cossi, M. *J. Phys. Chem. A* **1998**, *102*, 1995.
(33) (a) Car, R.; Parrinello, M. *Phys. Rev. Lett.* **1985**, *55*, 2471. (b) Laasonen, K.; Pasquarello, A.; Car, R.; Lee, C.; Vanderbilt, D. *Phys. Rev. B* **1993**, *47*, 10142.
(34) *CPMD-3.9.2*; Copyright IBM Corp 1990−2006, Copyright MPI für Festkörperforschung Stuttgart 1997−2001.
(35) Vanderbilt, D. *Phys. Rev. B* **1990**, *41*, 7892.

Table 3. Solvation Free Energies, Relative Solvation Free Energies (kcal/mol), and Cavity Volumes (Å^3) Computed with CPCM at the PBEPBE and MP2 Levels of Theory Using Basis-Sets Combinations ***A*** and ***B***

	H	$\mathbf{P_P}$	$\mathbf{P_T}$	**T**
PBEPBE/***A***				
ΔG_{solv}	−73.34	−68.97	−73.25	−59.41
$\Delta(\Delta G_{solv})$	0.00	4.36	0.08	13.92
V	157.6	163.6	156.9	180.5
PBEPBE/***B***				
ΔG_{solv}	−70.59	−67.01	−71.11	−57.77
$\Delta(\Delta G_{solv})$	0.00	3.58	−0.52	12.82
V	160.0	164.0	157.3	181.1
MP2/***A***				
ΔG_{solv}	−71.09	−65.67	−68.42	−63.11
$\Delta(\Delta G_{solv})$	0.00	5.43	2.67	7.98
V	163.3	168.0	169.4	179.2
MP2/***B***				
ΔG_{solv}	−68.97	−63.74	−66.44	−61.59
$\Delta(\Delta G_{solv})$	0.00	5.23	2.53	7.37
V	163.7	168.0	169.3	178.2

MP2 method comes close to this situation, but the values reported in Tables 1 and 2 suggest that a pentacoordinated species is increasingly preferred as the basis set is expanded. Therefore, it seems that it is not possible to conclude in favor of particular coordination number for vanadium on the basis of gas-phase calculations without having at hand the results of a higher theoretical model.

However, because the experimental conclusions come from solution chemistry studies, we have investigated the influence of the solvent using a simple polarizable continuum model (CPCM). Table 3 contains the results computed using the PBEPBE functional and second-order Möller−Plesset perturbational theory for the calculations of hydration enthalpies. It is immediately seen that taking into account the solvent effects plays an important role in the relative stabilities. Indeed, at the PBEPBE level of theory, the **T** conformation switches from the most stable in the gas phase to the least stable in aqueous solution. However, the **H** and $\mathbf{P_T}$ geometries undergo a stronger stabilization due to hydration, with the corresponding ΔG_{solv} values being nearly equal. Given the gas-phase free-energy ordering, the $\mathbf{P_T}$ structure therefore becomes the unambiguously preferred one with two basis-sets combinations. It should be pointed out that the computed ΔG_{solv} values correlate rather well for such charged species with molecular cavity volumes evolution (Table 3). Because we have a tetracoordinated structure that is significantly less compact than the $\mathbf{P_T}$ one, the electrostatic contributions are therefore lower in the former than in the latter and induce a weaker stabilization in that case. We note that incorporating the solvent effect gives the $\mathbf{P_T} < \mathbf{H} < \mathbf{P_p} < \mathbf{T}$ ordering using the PBEPBE functional. The case of the $\mathbf{P_T}$ conformation deserves additional comments, because it breaks the qualitatively expected cavity volume sequence, which is otherwise satisfying, and hence the putative stability classification as a function of the vanadium coordination number. Indeed, for the two five-coordinated species, the computed volumes are rather different and, so are the ΔG_{solv} values. Surprisingly enough, the $\mathbf{P_T}$ volumes determined for both basis sets are even lower than the hexacoordinated ones. From a quantitative point of view, the $\mathbf{P_T}$ volumes are more than 6.5 Å^3 lower than the ones associated with the $\mathbf{P_P}$ conformation, and increased stabilizations of $\mathbf{P_T}$ versus $\mathbf{P_P}$ equal to 4.3 and 4.1 kcal/mol have therefore been computed for the ***A*** and ***B*** basis sets, respectively. A more in-depth discussion concerning this peculiar but important point will be carried out subsequently.

Turning to the MP2 results, a clear preference for the hexacoordinated species with respect to the other structures is observed using both basis-sets combinations, which is in agreement with the experimental proposal. It should be noted that the corresponding stability ordering qualitatively mimics the one already determined on the basis of only the total electronic energies. However, the result obtained including the solvation free energy appears to be much more satisfying, because the stability sequence $\mathbf{H} < \mathbf{P_T} \approx \mathbf{P_P} < \mathbf{T}$ closely matches the number of ligands bonded to the vanadium metal center. Indeed, the two pentacoordinated structures can be considered as almost energetically equivalent and are located more than 5.5 kcal/mol below and 4.0 kcal/mol above the **T** and **H** conformations, respectively. Let us point out that the MP2-computed ΔG_{solv} values exhibit larger deviations from the cavity volume−free hydration energy correlation with respect to the above-presented DFT results, presumably because of the fact that the solvent reaction field for PCM MP2 calculations is computed on the basis of the HF solute electronic density. Indeed, for the $\mathbf{P_T}$ and $\mathbf{P_P}$ geometries, where the differences in volumes are lower than 1.5 Å^3 with the two basis sets, an overstabilization of the $\mathbf{P_T}$ conformation equal to approximately 2.8 kcal/mol could be computed.

Examination of the MP2 and PBEPBE data shows that the remaining discrepancy between those two types of calculations appears to be solely related to the $\mathbf{P_T}$ structure; more precisely, to the too small cavity volume associated with this geometry. To check if the problem is intrinsic to DFT-type calculations, or related to the nature of the functional employed, additional calculations have been carried out with the extended basis-sets combination only, using different functionals along the DFT Jacob's ladder proposed by Perdew. Indeed, we have used the well-known BP86 gradient-corrected functional like the PBEPBE one corresponding to the second rung. Moreover, two hybrid-GGA functionals were employed, namely, PBE1PBE and mPW1PW91. Finally, the recently introduced B1B95 and mPW1B95 meta-GGA hybrid functionals were also used to optimize and compute the hydration energy. The corresponding results are summarized in Table 4. It is immediately seen that the "old generation" BP86 and "new generation" PBEPBE functional results are equivalent with respect to the ordering of the energetical stabilities and cavity volumes. Similarly, the two hybrid-GGA calculations can be grouped together. This holds also true for the two hydrid-meta-GGA functionals. More importantly, we observe that as soon as some HF exchange is introduced the $\mathbf{P_T}$ volume becomes much more in-line with the $\mathbf{P_P}$ one, which in turn induces very close hydration-energy contributions for the two five-coordinated species. As a consequence, equivalent stability sequences equal to $\mathbf{H} < \mathbf{P_P} < \mathbf{P_T} < \mathbf{T}$ are obtained. Comparison with the MP2 result shows that an inversion of the two **P** geometries is still present, but this remaining

Table 4. Relative Energies (ΔE), Free Energies ($\Delta G°$), Solvation Free Energies, Relative Solvation Free Energies (kcal/mol), Cavity Volumes (Å^3), and Relative Free Energies in Solution Computed with CPCM Using MP2 and Various DFT Functionals with Basis-Sets Combination ***B***

	H	$\mathbf{P_P}$	$\mathbf{P_T}$	**T**	stability sequence
BP86					
ΔE	0.00	−4.39	−4.02	−6.63	$\mathbf{T < P_P \approx P_T < H}$
$\Delta G°$	0.00	−3.43	−4.40	−9.35	$\mathbf{T < P_T < P_P < H}$
ΔG_{solv}	−70.76	−67.19	−71.23	−58.19	
($\Delta(\Delta G_{solv})$	0.00	3.56	−0.48	12.57	
V	159.2	163.8	157.4	182.2	
$\Delta G° + \Delta(\Delta G_{solv})$	0.00	0.13	−4.88	3.22	$\mathbf{P_T < H \approx P_P < T}$
PBEPBE					
ΔE	0.00	−3.83	−3.36	−5.18	$\mathbf{T < P_P \approx P_T < H}$
$\Delta G°$	0.00	−2.99	−3.71	−8.24	$\mathbf{T < P_T < P_P < H}$
ΔG_{solv}	−70.59	−67.01	−71.11	−57.77	
$\Delta(\Delta G_{solv})$	0.00	3.58	−0.52	12.82	
V	160.0	164.0	157.3	181.1	
$\Delta G° + \Delta(\Delta G_{solv})$	0.00	0.59	−4.23	4.58	$\mathbf{P_T < H < P_P < T}$
PBE1PBE					
ΔE	0.00	−3.18	−1.91	−2.26	$\mathbf{P_P < T < P_T < H}$
$\Delta G°$	0.00	−2.83	−2.87	−6.23	$\mathbf{T < P_T \approx P_P < H}$
ΔG_{solv}	−71.41	−67.28	−66.82	−57.96	
$\Delta(\Delta G_{solv})$	0.00	4.13	4.58	13.45	
V	156.9	162.6	162.7	180.6	
$\Delta G° + \Delta(\Delta G_{solv})$	0.00	1.30	1.71	7.22	$\mathbf{H < P_P \approx P_T < T}$
PBEPBE//PBE1PBE1					
ΔG_{solv}	−70.35	−66.38	−65.77	−57.11	
$\Delta(\Delta G_{solv})$	0.00	3.97	4.58	13.25	
mPW1PW91					
ΔE	0.00	−3.36	−2.20	−3.04	$\mathbf{P_P \approx T < P_T < H}$
$\Delta G°$	0.00	−3.01	−3.32	−6.83	$\mathbf{T < P_T \approx P_P < H}$
ΔG_{solv}	−71.21	−67.18	−66.82	−58.02	
$\Delta(\Delta G_{solv})$	0.00	4.04	4.39	13.20	
V	156.9	162.7	163.2	181.1	
$\Delta G° + \Delta(\Delta G_{solv})$	0.00	1.03	1.08	6.37	$\mathbf{H < P_P \approx P_T < T}$
B1B95					
ΔE	0.00	−1.57	−0.29	0.70	$\mathbf{P_P < P_T \approx H < T}$
$\Delta G°$	0.00	−2.35	−1.69	−4.04	$\mathbf{T < P_P < P_T < H}$
ΔG_{solv}	−71.26	−66.57	−66.27	−61.55	
$\Delta(\Delta G_{solv})$	0.00	4.69	4.99	9.72	
V	156.9	163.0	163.2	172.9	
$\Delta G° + \Delta(\Delta G_{solv})$	0.00	2.34	3.31	5.68	$\mathbf{H < P_P < P_T < T}$
mPW1B95					
ΔE	0.00	−1.14	0.37	2.28	$\mathbf{P_P < H \approx P_T < T}$
$\Delta G°$	0.00	−1.84	−1.22	−2.83	$\mathbf{T < P_P < P_T < H}$
ΔG_{solv}	−71.76	−66.98	−66.63	−61.51	
$\Delta(\Delta G_{solv})$	0.00	4.77	5.13	10.24	
V	156.1	162.6	162.5	171.8	
$\Delta G° + \Delta(\Delta G_{solv})$	0.00	2.93	3.91	7.41	$\mathbf{H < P_P < P_T < T}$
MP2					
ΔE	0.00	0.20	4.10	8.40	$\mathbf{H \approx P_P < P_T < T}$
$\Delta G°$	0.00	−0.83	1.51	2.57	$\mathbf{P_P < H < P_T < T}$
ΔG_{solv}	−68.97	−63.74	−66.44	−61.59	
$\Delta(\Delta G_{solv})$	0.00	5.23	2.53	7.37	
V	163.7	168.0	169.3	178.2	
$\Delta G° + \Delta(\Delta G_{solv})$	0.00	4.40	4.04	9.94	$\mathbf{H < P_T \approx P_P < T}$

difference can be considered as anecdotal, given that the free-energy gap between the pentacoordinated species, incorporating solvation, amounts for less than 1 kcal/mol.

One of the main conclusions that can be drawn from the above investigation is that taking into account solvent effects cannot be avoided for the energy classification of solvated charged species using DFT calculations. A second conclusion is that *pure* gradient-corrected functionals appear to be somewhat insufficient when trying to get some clues concerning a complex experimental problem such as transition-metal hydration on the basis of such small-sized model clusters where hydrogen bonds might be present. It is indeed well-known that DFT calculations, especially *pure* functionals, are less accurate than MP2 for hydrogen-bonded systems because of an incomplete description of long-range dispersion forces while at the same time giving better metal−ligand bond distances. For charged systems where electrostatic contributions dominate, this discrepancy may be partly hidden. In our case, it seems however that some problems with *pure* functionals remain with our simple models. Examination of the hydrogen bond distances (Supporting Information) shows that almost all of the DFT values are significantly shorter than the MP2 ones. In the case of conformations with sensitive terminal hydrogen-bonded water molecules, as in the $\mathbf{P_T}$ and **T** structures, the difference reaches up to ∼0.14 Å in the case of the BP86 and PBEPBE functionals. Upon climbing the DFT Jacob's ladder, this difference drops by up to ∼0.06 Å, the best correction of this delicate parameter being obtained with the two hybrid-meta-GGA functionals. Therefore, we believe that the excessive stabilization of the $\mathbf{P_T}$ structure due to hydration is *only* a geometrically related issue, that is, an incorrectly computed cavity volume that is indirectly a consequence of the insufficiently accurate $\mathbf{P_T}$ structure determined at the PBEPBE or BP86 levels of theory rather than due to an incorrect calculation of ΔG_{solv} values by pure gradient-corrected functionals. To test this assumption, we have carried out calculations at the PBEPBE/B//PBE1PBE/B level of theory (Table 4), where the cavity volumes derived from the PBE1PBE-optimized geometries for the two pentacoordinated conformations can be considered as equal. Comparison with the PBEPBE/B//PBEPBE/B results shows that the solvation energy of the $\mathbf{P_T}$ conformation would be reduced by 5.3 kcal/mol, whereas the other ΔG_{solv} values are almost unaffected and therefore lead to the $\mathbf{H < P_T \approx P_P < T}$ sequence.

We note that the final energy differences $\mathbf{H - P}$ are rather low, at least with hybrid-GGA functionals, which suggests that both six- and five-coordinated structures may coexist at room temperature. Meanwhile, the tetrahedral form is expected to be less plausible. Such remarks obviously do not consider the energy perturbations that may induce hydrogen bonds between solute and explicit solvent molecules. Furthermore, from a strictly speaking geometrical point of view, those bonds are expected to be longer than those in our $\mathbf{P_T}$ simple model, for example, because of the dense network of hydrogen bonds between the bulk solvent and the first solvation shell, as well as within this hydration sphere. Indeed, we have observed in an earlier theoretical study an increase, equal to 0.18 Å, in the corresponding hydrogen bond lengths on going from $[V(H_2O)_6]^{2+}\cdot H_2O$ to $[V(H_2O)_6]^{2+}\cdot(H_2O)_{12}$.[36] Thus, we are confident that the volume artifact that occurs concerning one of the $[VO_2(H_2O)_4]^+$ conformations using PCM with pure DFT static calculations does not preclude the use of the PBEPBE functional, provided that an improved solvent model is employed, consisting, for example, of at least a full second hydration shell around the complexes. In the next section,

(36) Benmelouka, M.; Messaoudi, S.; Furet, E.; Gautier, R.; Le Fur, E.; Pivan, J.-Y. *J. Phys. Chem. A* **2003**, *107*, 4122.

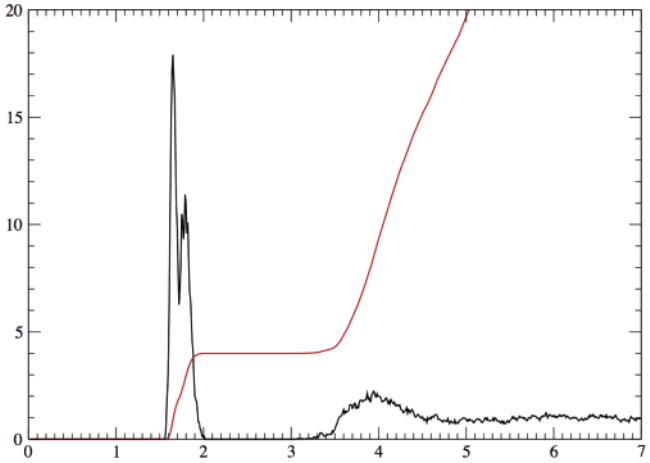

Figure 2. V−O radial distribution function and its integration computed over the last 6 ps of the molecular dynamics simulation at 300 K, starting from $VO_2(H_2O)_4^+$ in a neutral aqueous solvent.

we will precisely describe the results of an investigation using an explicit solvent carried out by means of Car−Parrinello molecular dynamics.

The system was built up from scratch and consists of one $VO_2(H_2O)_4^+$ complex surrounded by 28 water molecules. The simulation was carried out in the microcanonical ensemble (NVE) for 18 ps following an equilibration phase of 1 ps. Examining the evolution of the various M−O bond distances in the complex reveals that one of the two most labile water molecules located trans to an oxo ligand is expelled after 4.3 ps. Approximately 6 ps later, the departure of another ligand is observed. Therefore, we have at hand a tetracoordinated structure that is kept until the end of the simulation. In the study carried out by Bühl and Parrinello using Troullier−Martins pseudopotentials and the BLYP functional, the same $VO_2(H_2O)_3^+$ was already detected following a similar reaction pathway. However, a tetrahedral arrangement around the vanadium was not observed during the 2 ps simulations that were sufficient for the purpose of their investigations. In our case, the four-coordinated geometry conservation is clearly apparent in Figure 2 containing the V−O radial distribution function and its integration, labeled here as g(V−O) and n(V−O), respectively, that were computed from the last 6 ps of the simulation. Indeed, n(V−O) reaches a plateau for distances, between ∼2 and ∼3.5 Å, associated with the presence of four oxygen atoms in the vanadium coordination sphere. For shorter distances, a small shoulder corresponding roughly to n(V−O) = 2 is also visible and can be attributed to the oxo ligands. The presence of those strongly bonded ligands is unambiguously seen in the g(V−O) plot, which exhibits a sharp spike centered around 1.65 Å that is clearly separated from a second maximum showing some kind of substructure, centered around 1.78 Å. Finally, the solvent organization around the solute and the exchange of water molecules between the first solvation sphere and the bulk solvent is depicted by a large maximum located at ∼4 Å that does not fall to zero above 4.5 Å. This hydration sphere can be estimated to contain on average 10 water molecules.

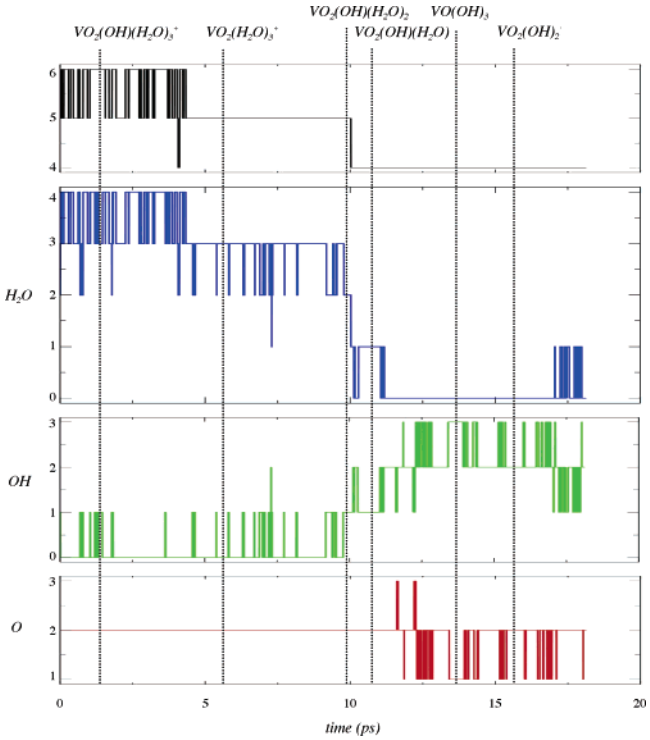

Figure 3. Evolution (bottom to top) of the number of oxo, hydroxo, and water ligands and coordination number of vanadium in a Car−Parrinello simulation in aqueous solution at 300 K, starting from $VO_2(H_2O)_4^+$.

A closer examination of the vanadium coordination sphere in our calculation shows that changes occurred concerning not only the number but also the nature of the ligands. Figure 3 summarizes the results obtained concerning the evolution of the coordination number together with the total numbers of oxo, hydroxo, and water ligands bonded to the vanadium. The distance criterions used to obtain those drawings were determined from the V−O and O−H radial distribution functions for the simulation. As suggested by the analysis of the M−O bond distances, an equilibrium between $VO_2(H_2O)_3^+$ and $VO_2(H_2O)_4^+$ characterizes the first 4 ps of the simulation. Several reversible deprotonations of mainly axial water molecules have also been detected in the meantime (Figure 3). This last process continues during the following 6 ps and becomes irreversible, leading to $VO_2(OH)(H_2O)_2$ approximately 200 fs, before switching to a tetracoordinated structure because of the departure of the second water molecule located trans to the oxo. Finally, at t = 11.1 ps, a second deprotonation of the remaining water molecule occurs, which gives $VO_2(OH)_2^-$. This structure is largely predominant until the end of the simulation as seen in Figure 3. We note that $VO(OH)_3$ has also been detected after protonation of one of the oxo ligands of $VO_2(OH)_2^-$. This structure appears, however, relatively short-lived at 300 K. The longest lifetime computed from our plot corresponds to about 0.5 ps around t = 13.4 ps. During this last phase of the calculation where only a tetracoordinated structure is present, several proton exchanges between the solute and the solvent have been detected. Such a mechanism adds some flexibility in the hydroxyl ligands' position and may therefore have some consequences on the formation processes of vanadophosphates.

While corresponding to an a priori surprisingly important modification of the vanadium coordination sphere on the time scale of our simulation, the evolution from VO_2^+ to $VO_2(OH)_2^-$ described above seems to be in qualitative agreement with the pH/concentration diagram given in Figure 1. To carry out this comparison, we shall only take into account the part of the diagram associated with the mononuclear species, because the formation of polyvanadates resulting from the condensation of those complexes is impossible in our simulations from a technical point of view. On the one hand, the VO_2^+ cation appears to be stable at room temperature, in the presence of a sufficiently acidic solvent, that is, for experimental pH values lower than 3.5, with a predominance domain that is extended upon a H_3O^+ concentration increase. On the other hand, when the tiny zone attributed to H_3VO_4 covering only 0.5 pH unit is neglected, the adjacent predominance domain ranging from approximately pH 4 to 8 pertains to the $VO_2(OH)_2^-$ complex. Therefore, because we have initially built up $VO_2(H_2O)_4^+$ in a neutral medium, the observed system evolution toward $VO_2(OH)_2^-$ for the duration of our simulation does not appear to be inconsistent, while at the same time it does not preclude the possibility of a transient recovery of the solvated VO_2^+ cation, provided that simulations could be done for a much longer time scale. Finally, we point out that we do not expect the decomposition process leading from VO_2^+ to $VO_2(OH)_2^-$ to follow exactly the same sequence of steps, despite the fact that a similar reaction pathway was also obtained using different calculation parameters.[37] In that case, the $VO_2(OH)_2^-$ complex is also the resulting predominant species.

In our laboratory, the synthesis of vanadophosphates generally involves high phosphoric acid concentrations that induce typical pH values that are lower than 2. To simulate the acidity of the medium, we formed four hydronium ions in a simulation cell constructed in a fashion similar to that in the neutral case (i.e., $VO_2(H_2O)_4^+$ surrounded by 28 solvent molecules). This choice of adding four protons was guided by the fact that in the previous calculation two hydronium ions were present in the medium as a result of $VO_2(OH)_2^-$ formation.[38]

The Car−Parrinello calculation was carried out for 24 ps in the NVE ensemble after 1 ps of equilibration. By the end of this preliminary phase, the $VO_2(H_2O)_3^+$ species is obtained. During the early steps of the production phase, a competition between penta- and hexacoordinated complexes occurs, suggesting a possible return to $VO_2(H_2O)_4^+$. After 3.3 ps, however, the coordination sphere of VO_2^+ stabilizes to three water molecules, and the five-coordinated arrangement is almost exclusively observed during the remaining 21 ps of the simulation (V−O radial distribution function reported in the Supporting Information). An analysis shows indeed only one reversible event of approximately 100 fs at $t = 7.6$ ps where a tetracoordinated structure has be detected. An enhanced stability of the vanadium coordination sphere can also been noted, with the only significant transitory events concerning reversible deprotonations of the water molecules. This clear preference for a VO_2^+ cation in an acidic medium at room temperature is in overall qualitative agreement with the experimental data presented in Figure 1. However, in contrast to the suggestion made by Cruywagen et al.,[15] we do not observe $VO_2(H_2O)_4^+$ but $VO_2(H_2O)_3^+$ as the major species. Generally speaking, $VO_2(H_2O)_n^+$ complexes cannot constitute viable precursors from the point of view of the nucleation processes of vanadophosphates. They indeed lack the hydroxyl ligands required to build oxo bridges by means of oxolation reactions.

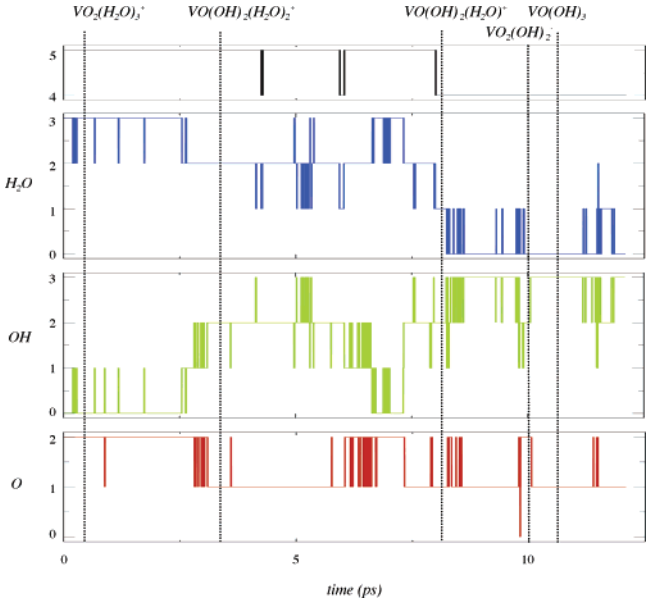

Figure 4. Evolution (bottom to top) of the number of oxo, hydroxo, and water ligands and coordination number of vanadium in a Car−Parrinello simulation in aqueous solution at 500 K, starting from $VO_2(H_2O)_3^+$ in an acidic medium.

An investigation of the temperature influence on VO_2^+ stability in an acidic medium was therefore carried out. The starting configuration was taken after 6 ps of the previous run and heated to 500 K by velocity scaling during another 1 ps of equilibration. This value corresponds to the average temperature used for the hydrothermal synthesis of vanadophosphates in our laboratory. The production phase was subsequently carried out for 12 ps, leading to an average temperature for the simulation of 472 K. Figure 4 presents the evolution of the system during the production phase. It is immediately seen that the most striking feature is related to the loss of the five-coordinated structure after 8 ps. During that period, $VO_2(H_2O)_3^+$ disappears in the 2.5−6.7 ps interval

(37) A Car−Parrinello test simulation performed at an average temperature of 440 K, using a different initial configuration and Troullier−Martins pseudopotentials with a kinetic energy cutoff of 80 Ry has displayed the switch to $VO_2(H_2O)_3^+$ within the first 0.5 ps of the production phase probably because of the higher temperature. Evolution to $VO_2(OH)(H_2O)$ occurs around 6.5 ps through the nearly simultaneous deprotonation of an axial water molecule and elimination of an equatorial water ligand. This process is followed approximately 0.4 ps later by the formation of $VO_2(OH)_2^-$, which is kept almost exclusively over the remaining 1.9 ps of the calculation.

(38) In an alternative approach, we placed a naked V^{5+} ion in one cavity of a water box containing 32 molecules. The obvious advantage of this method is that we do not impose a specific structure to the vanadium complex. The simulation showed the spontaneous formation of a $VO_2(H_2O)_3^+$ complex with a *cis*-VO_2^+ core, after only 170 fs, together with the simultaneous acidification of the solvent because of formation of four H_3O^+.

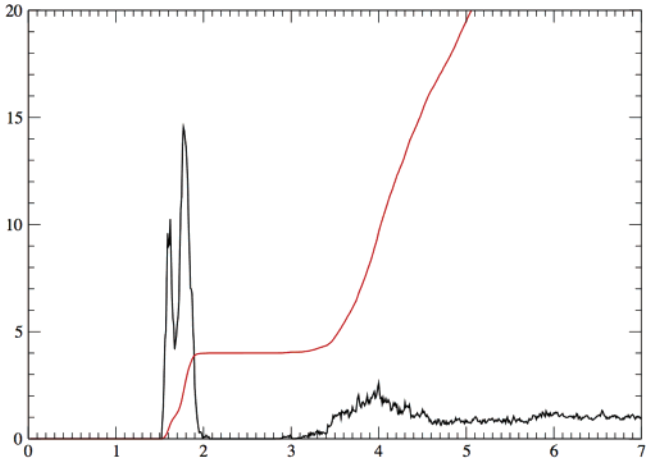

Figure 5. V−O radial distribution function and its integration computed over the last 4 ps of the molecular dynamics simulation at 500 K, starting from $VO_2(H_2O)_3^+$ in a strongly acidic aqueous solvent.

of time, after deprotonation of one water molecule that will be followed approximately 0.6 ps later by protonation of an oxo ligand. The complex $VO(OH)_2(H_2O)_2^+$ resulting from this proton exchange is almost the exclusive species until $VO_2(H_2O)_3^+$ is recovered by an inverse process involving exactly the same oxygen atoms, leading to a status quo ante bellum. Deeper changes occur starting at $t = 7.3$ ps when the second oxo and one of the previously unaffected water molecules undergo a similar but faster proton exchange that gives an alternative $VO(OH)_2(H_2O)_2^+$ structure in which the two water molecules are located trans to each other. The switch to a tetracoordinated environment occurs 0.7 ps later, with one of the remaining water molecules expelled in the bulk solvent. Therefore, we have at hand a complex that already possesses two hydroxyl ligands ready to form two oxo bridges through oxolation reactions. We note that a closely related mechanism was also found when a different approach[38] was used to construct an acidified simulation cell. We indeed observed the nearly simultaneous formation of two hydroxyl groups resulting from protonation of an oxo ligand and deprotonation of a water ligand with the subsequent elimination of one water molecule that leads to the tetracoordinated species $VO(OH)_2(H_2O)^+$. During the last 4 ps of the simulation (Figures 4 and 5), the tetrahedral arrangement is kept, but more importantly, the predominant structure corresponds to a neutral $VO(OH)_3$ molecule in equilibrium mainly with $VO_2(OH)_2^-$ ($t = 9.8-10.1$ ps) and $VO(OH)_2(H_2O)^+$ ($t = 8.0-8.3$ and 11.5−11.8 ps). We point out that the H^+ exchange process involved in the $VO(OH)_3/VO_2(OH)_2^-$ equilibrium might induce a modification of the oxo position, because nothing ensures reprotonation on the same oxygen atom. Such a mechanism therefore gives some kind of flexibility to the oxo ligand position during inorganic polymerization involving the $VO(OH)_3$ precursor.

Turning back to Figure 1, we observe that $VO(OH)_3$ is confined at room temperature in a very narrow range of 0.5 pH units centered on 3.5. As pointed out in the Introduction, several authors had to reconsider the very existence of this particular species.[9,16] Our calculations suggest, however, that $VO(OH)_3$ may probably be preferred in an acidic aqueous medium around 500 K over a broader range of pH values and that it therefore possesses an intrinsic stability in conditions trying to simulate those of hydrothermal synthesis. This result appears to be encouraging from the point of view of the rationalization of the nucleation and growth processes of solid compounds such as $VOPO_4 \cdot 2H_2O$. Indeed, the $VO(OH)_3$ precursor may already be able to form three of the four oxo bridges with three H_3PO_4 molecules by oxolation reactions.

Finally, it should be pointed out that this work could be used as a preliminary step to carry out subsequent calculations using much larger simulation cells and/or incorporating counterions to tune more precisely the pH parameter and/or study the influence of counterions on the reaction processes, respectively, so that a finer picture of V(V+) speciation under hydrothermal conditions is obtained.

Conclusions

Static quantum chemical calculations and Car−Parrinello molecular dynamics simulations have been carried out to investigate the structure and stability of VO_2^+ in aqueous solution. Static calculations on $[VO_2(H_2O)_{(4-n)}]^+ \cdot nH_2O$ ($n = 0-2$) conformers showed that solvent effects had to be taken into account using for example the CPCM model to restore agreement between hybrid DFT and MP2 calculations for a hexacoordinated vanadium environment, whereas the gas-phase free-energy results using our extended basis-sets combination gave a preference for the four-coordinated and one of the five-coordinated structures, respectively. Using this first level of solvation treatment led to the conclusion that $VO_2(H_2O)_4^+$ and $VO_2(H_2O)_3^+$ were, however, almost as stable with hybrid functionals, which is somewhat at variance with the experimental suggestion of Cruywagen et al., whereas at the MP2 and hybrid-meta-GGA DFT levels of theory, the preference is less ambiguous. A discussion of the parameters that lead to an excessive hydration stabilization of the pentacoordinated geometry with a terminal water molecule using pure DFT-type calculations has been carried out. We have shown that this discrepancy can be related to a too small cavity volume for the $\mathbf{P_T}$ structure. This geometrical problem is an indirect consequence of the less accurate description of presumably the hydrogen bonds with respect to DFT calculations incorporating some amount of HF exchange.

Car−Parrinello simulations using explicit water molecules have allowed us to conclude that acidification of the solvent was of paramount importance to avoid the spontaneous evolution from VO_2^+ to the $VO_2(OH)_2^-$ complex preferred under neutral conditions, on the time scale of the calculations. In that case only, the relative stability of $VO_2(H_2O)_4^+$ and $VO_2(H_2O)_3^+$ could be investigated up to 24 ps, giving the pentacoordinated species as largely predominant. The simulation carried out at 500 K in an acidic medium has led to the conclusion that $VO(OH)_3$ was the most stable species under those emulated hydrothermal synthesis conditions, whereas its very existence at room temperature was not clearly established. We believe that this structural analogue

of H_3PO_4 therefore undergoes a stability domain enlargement because of the temperature increase.

Acknowledgment. We thank IDRIS-CNRS (Orsay) and CINES-MENESR (Montpellier) for providing access to their computational facilities.

Supporting Information Available: Gas-phase-optimized geometries of $[VO_2(H_2O)_{(4-n)}]^+ \cdot nH_2O$ ($n = 0-2$) at the BP86/***B***, PBEPBE/***A*** and ***-B***, PBE1PBE/***B***, mPW1PW91/***B***, B1B95/***B***, mPW1B95/***B***, and MP2/***A*** and ***-B*** levels of theory; gas-phase-optimized geometries and relative stabilities of $[VO_2(H_2O)_{(4-n)}]^+ \cdot nH_2O$ ($n = 0-2$) as test calculations of the ultrasoft pseudopotentials employed in the CPMD calculations; and V−O radial distribution function and its integration for the CPMD simulation at 300 K, in an acidic medium. This material is available free of charge via the Internet at http://pubs.acs.org.

IC0614519